Astron. Astrophys. 359, 941–947 (2000)

ASTRONOMY AND ASTROPHYSICS

ISO detection of a 60 μm source near GRB 970508

L. Hanlon[1], R.J. Laureijs[2], L. Metcalfe[2], B. McBreen[1], B. Altieri[3], A. Castro-Tirado[4,5], A. Claret[6], E. Costa[7], M. Delaney[1,8], M. Feroci[7], F. Frontera[9], T. Galama[10], J. Gorosabel[4], P. Groot[10], J. Heise[11], M. Kessler[2], C. Kouveliotou[12], E. Palazzi[9], J. van Paradijs†[10,13], L. Piro[7], and N. Smith[14]

[1] Department of Experimental Physics, University College Dublin, Belfield, Stillorgan Road, Dublin 4, Ireland
[2] ISO Data Centre, Astrophysics Division, ESA, Villafranca, Spain
[3] XMM Data Centre, Astrophysics Division, ESA, Villafranca, Spain
[4] Laboratorio de Astrofísica Espacial y Física Fundamental, Villafranca del Castillo, P.O. Box 50727, 28080 Madrid, Spain
[5] Instituto de Astrofísica de Andalucía (IAA-CSIC), P.O. Box 03004, 18080 Granada, Spain
[6] Service d'Astrophysique, CEA/DSM/DAPNIA Saclay, Orme des Merisiers, 91191 Gif-sur-Yvette Cédex, France
[7] Istituto Astrofisica Spaziale, CNR, 00133 Roma, Italy
[8] Stockholm Observatory, 133 36 Saltsjöbaden, Sweden
[9] ITESRE-CNR, Bologna, Italy
[10] Astronomical Institut 'Anton Pannekoek', University of Amsterdam, Amsterdam, The Netherlands
[11] SRON Utrecht, The Netherlands
[12] USRA at NASA/MSFC, Huntsville AL, USA
[13] Physics Department, University of Alabama, Huntsville, USA
[14] Department of Applied Physics and Instrumentation, Cork Institute of Technology, Cork, Ireland

Received 25 April 2000 / Accepted 9 May 2000

Abstract. The Infrared Space Observatory observed the field of the γ–ray burst GRB 970508 with the CAM and PHT instruments on May 21 and 24, 1997 and with PHT in three filters in November 1997. A source at 60 μm (flux in May of 66 ± 10 mJy) was detected near the position of the host galaxy of this γ–ray burst. The source was detected again in November 1997, at a marginally lower flux (43 ± 13 mJy). A Galactic cirrus origin and a stellar origin for the emission can be ruled out on the basis of the infrared colours. The marginal evidence for variability in the 60 μm flux between May and November is not sufficient to warrant interpretation of the source as transient fireball emission. However, the infrared colours are physically reasonable if attributed to conventional dust emission from a single blackbody source. The probability of detecting a 60 μm source by chance in a PHT beam down to a detection limit of 50 mJy is $\sim 5 \times 10^{-3}$. If the source is at the redshift of the host galaxy of the γ–ray burst the fluxes and upper limits at wavelengths from 12 μm to 170 μm indicate it is an ultraluminous infrared galaxy ($L_{ir} \sim 2 \times 10^{12} L_{\odot}$). The star formation rate is estimated to be several hundred solar masses per year, depending significantly on model-dependent parameters. If this source is associated with the host galaxy of GRB 970508, progenitor models which associate GRBs with star-forming regions are favoured.

Key words: gamma rays: bursts – gamma rays: observations – infrared: galaxies – infrared: general – ISM: dust, extinction

Send offprint requests to: L. Hanlon (lhanlon@bermuda.ucd.ie)

1. Introduction

The recent discoveries of fading afterglows to a number of γ–ray bursts (GRBs) have been precipitated by the accurate and prompt localisation capability of the two Wide Field Cameras (WFC) aboard the 'BeppoSAX' X-ray satellite (Boella et al. 1997; Piro et al. 1998a). The typical $\sim 3'$ radius error circles, obtained in a matter of hours after the occurrence of the GRBs, are easily covered by ground-based optical and radio telescopes, allowing rapid and deep follow-up observations. The reduction of GRB error circles by BeppoSAX also made it feasible to study the content of these regions at far-infrared wavelengths with the European Space Agency's Infrared Space Observatory[1], ISO (Kessler et al., 1996). The error region of GRB 970402 was the first to be rapidly surveyed at far-infrared wavelengths (Castro-Tirado et al., 1998a). ISO observed this GRB error circle 55 hours, and again 8 days, after the burst event and detected no new transient sources down to a 5σ limit of 0.14 mJy at 12 μm and 350 mJy at 170 μm. Details of the ISO observations of GRBs may be found in Delaney et al. (1999) .

2. Observations of GRB 970508

GRB 970508 triggered the GRB Monitor (Frontera et al., 1997) of BeppoSAX at 21:41:47 UT on May 8, 1997 (Costa et al., 1997). The GRB localisation was subsequently improved by the BeppoSAX WFC2 detector to a $3'$ radius

[1] Based on observations with ISO, an ESA project with instruments funded by ESA Member States (especially the PI countries: France, Germany, the Netherlands and the United Kingdom) with the participation of ISAS and NASA.

(99% confidence) error circle (Heise et al., 1997). Follow-up observations by the BeppoSAX narrow-field instruments (NFI) then detected a new, fading X–ray source, consistent with the GRB error circle, but with an improved positional accuracy of 50″ radius (Piro et al. 1998b). Within this error circle an optical transient (OT) was discovered whose flux increased for the first two days and subsequently decayed (Bond, 1997; Djorgovski et al., 1997). The decay phase was characterised by a power law dependence with time, $f(t) \propto t^{-1.1}$ days (Castro-Tirado et al., 1998b). Near-infrared (2.2μm) emission was also observed from the OT source between May 13.25 (K_s = 18.2$\pm$0.2 mag) and May 20.21 (K_s = 19$\pm$0.3 mag) (Chary et al., 1998). Spectra of the OT taken with the Keck II 10 m telescope revealed the presence of [OII] emission and FeII and MgII absorption lines consistent with a source at a redshift of 0.835, providing the first direct measurement of the distance to a GRB (Metzger et al. 1997a,b). Radio afterglow was also detected from a source at the position of the OT (Frail et al., 1997; Bremer et al., 1998; Galama et al., 1998). Observations by HST have shown the OT position to be remarkably well-centred with respect to the host galaxy (Fruchter et al., 1999). The host is late-type, with the characteristics of a blue compact galaxy (Sokolov et al., 1999).

We report here on ISO observations of the field of GRB 970508 in the weeks following the GRB and on a follow-up observation made in November 1997.

3. ISO Observations

The GRB 970508 error circle was not initially visible with ISO due to orbital constraints but became visible for seven short windows lasting from 3000 to 8500 seconds between May 20 and May 26, during which time target of opportunity observations were made with ISOCAM (Cesarsky et al., 1996) and ISOPHOT (Lemke et al., 1996). A second window was available from October 25 to November 21 1997 and follow-up observations were then made with ISOPHOT. Details and results from the CAM observations are presented elsewhere (Hanlon et al., 1999). The May observations were centred at RA(2000): 6 h 53 m 46.7 s, Dec(2000): +79° 16′ 02.0″, the centre of the X–ray afterglow error circle (Piro et al., 1998a). The November observations were centred on the position of the optical transient associated with the GRB (Bond, 1997).

Raster maps of the NFI 50″ radius error circle were obtained with the PHT C100 and C200 detectors (Klaas et al., 1994). The PHT C100 camera is a 3×3 pixel Ge: Ga array, with a pixel centre-to-centre distance of $46''$ in both directions. The C_60 filter (reference wavelength at 60 μm, width 23.9 μm) and the C_90 filter (reference wavelength at 90 μm, width 51.4 μm) are associated with the C100 detector. Observations in these filters employed a 5×5 position raster grid with a $23''$ step size in both directions. The grid was aligned with the orientation of the detector array. The size of the area covered was therefore $230'' \times 230''$. This mode of observing was selected to obtain a fully sampled map with a high level of redundancy in the map centre and to minimise the uncertainties due to cirrus confusion. The redundancy was highest in the inner $46'' \times 46''$ where it was 25. At 60 and 90 μm the FWHM of the beam profiles (psf convolved with pixel) are $41''$ and $47''$ respectively.

The PHT C200 camera is a 2×2 pixel stressed Ge: Ga array, with a pixel centre-to-centre separation of $92''$. A 5×5 grid raster with a $46''$ step size in both directions was used for the C200 observations in the C_160 filter band (reference wavelength at 170 μm, width 89.4 μm). The area covered was $368'' \times 368''$ with a redundancy for the inner $91'' \times 91''$ of 16.

4. ISOPHOT data processing

The ISOPHOT data were processed using the software package PIA version 7.3 (Gabriel et al., 1997). All standard processing steps were included to obtain the flux per raster point per detector pixel before map coaddition (Laureijs et al., 1998). This flux was taken to be the median value of all signals measured during a given raster point integration thereby minimising any positive flux bias due to the relatively high number of glitches, induced by ionising particles, in the data stream. The data were flatfielded by imposing the same integrated flux for all detector pixel scans. This operation yielded a correction factor for each pixel without affecting the total flux. The maps were constructed by coadding the flatfielded fluxes per raster point per detector pixel in a regular image grid of $23''\times23''$ image pixels which are aligned with the orientation of the detector pixels.

Photometry on the C_60 and C_90 maps was carried out by integrating the flux in an area of 5×5 image pixels, minus the corner pixels, in the region of interest and then subtracting the mean background flux derived from the remaining pixels in the map. The measured signal was then scaled up to the full PHT beam-size. Since the maps from May and November have different orientations and map centres, the 60 μm, 90 μm and merged (combined 60 μm and 90 μm) maps were reprojected to have the position of the OT as map centre and with zero position angle. These maps were used to derive photometric fluxes.

5. Results

A point source was detected at 60 μm on May 24, consistent with the OT position, given the uncertainty in the position of the peak of the beam profile with respect to the geometric shape of a given pixel (Fig. 1). For a relatively low signal to noise detection such as this (see Table 1), which is significant in only a few pixels (not all 9), an offset of even a few arcsec can cause the mapping routine to shift the source by an entire image pixel. However, it is possible that the offset of the source relative to the OT position is real and the consequences of this are discussed below. Further observations were made with PHT in November 1997 to verify the detection. The source was again detected at 60 μm (albeit at a lower significance level than in May) but no significant excess at the position of the OT was detected at 90 μm (see Fig. 2 and Table 1). Although the 60 μm flux is lower in November than in May, we do not regard this as providing strong evidence for variability, since the two fluxes agree to within 2σ. The offset of the source relative to the OT is again observed in the November

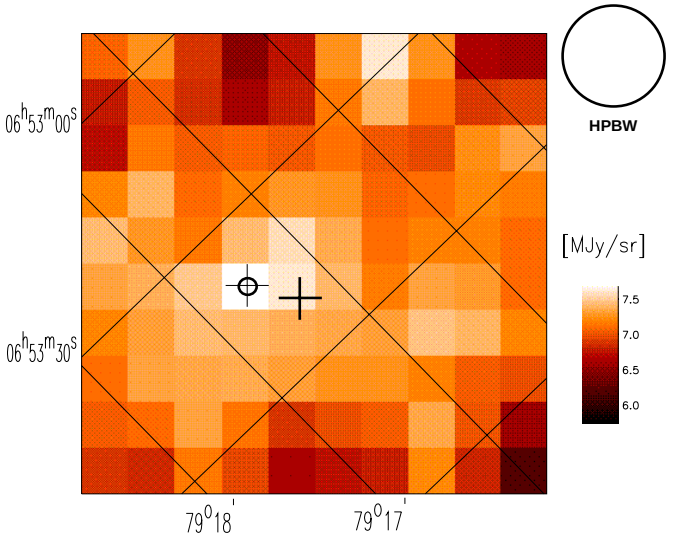

Fig. 1. PHT C100 map using the C_60 filter, taken on May 24, 1997. The OT position (marked with a cross) is consistent with the location of the C_60 source (marked with a circle) to within the HPBW of the C100 detector. The size of the HPBW is shown on the side of the figure, along with the grey scale values.

Table 1. Log of ISOPHOT observations of GRB 970508. The PHT fluxes correspond to the reprojected maps (see text for details).

UT Start - End	Instrument	Filter	Flux Density (mJy)
May 1997			
24.095 - 24.106	PHT	C_60	66 ± 10
24.107 - 24.114	PHT	C_160	< 70
November 1997			
11.021 - 11.040	PHT	C_60	43 ± 13
11.041 - 11.065	PHT	C_90	19 ± 7
11.066 - 11.070	PHT	C_160	< 130
Merged C_60 plus C_90			32 ± 9

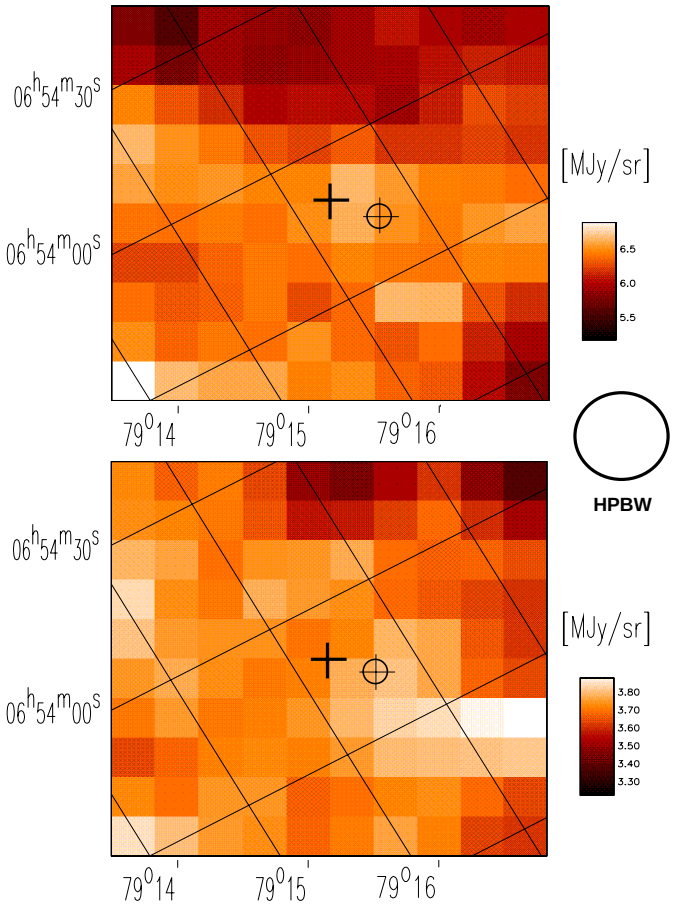

Fig. 2. PHT C100 map using the C_60 filter (top) and the C_90 filter (bottom), taken on November 11, 1997. The OT position is marked with a cross while the position of the C_60 source detected in May 1997 is marked with a circle. A source is present in the C_60 map which is consistent with both the position of the OT and the C_60 source detected in May 1997. Note: The orientation of these maps is different to that in Fig. 1, due to differences in orientation and map centres between the May and November observations.

map. In an attempt to improve the signal to noise ratio of the C100 observations from November 1997, the data from both filters were merged into a single map (Fig. 3). The 60 μm and 90 μm data were separately flatfielded and the corrected fluxes per pixel per detector and per filter were coadded on a common grid. The fluxes per filter were weighted by their respective uncertainties. The merged map has a noise level intermediate between the noise in the individual maps and the significance of this is discussed below. In addition, the source is detected at a signal to noise ratio consistent with that of the 60 μm map alone. This suggests that the source is not significant at 90 μm. Upper limits (3σ), derived from the 170 μm observations in May and November, are given in Table 1.

5.1. Assessment of uncertainties in the maps

Per raster point, the integration times were 20 s at 60 μm in the May observation and 60 s at 60 μm and 90 μm in the November observations. Although the integration time per raster point was three times longer at 60 μm in the second epoch, the noise levels per raster point in the two 60 μm maps are comparable (35 mJy/beam in May, 31 mJy/beam in November). The relative increase in the noise level of the C_60 measurement in November is most likely due to the fact that the observation was made at the end of a revolution and was therefore subject to an increased glitch rate as the satellite re-entered the radiation belts (Kessler et al., 1996). The noise level in the C_90 measurement was 17 mJy/beam. Including the redundancy, the predicted flux level in the map centre is about 12 mJy/beam at 60 μm and 6 mJy/beam at 90 μm.

The detection limit is also determined by the cirrus confusion noise (N), which can be estimated from

$$N(\mathrm{mJy}) = 1.08 \left(\frac{\lambda}{100\,\mu\mathrm{m}} \right)^{2.5} \times \left(\frac{I_\nu(\lambda)}{1\mathrm{MJy/sr}} \right)^{1.5}$$

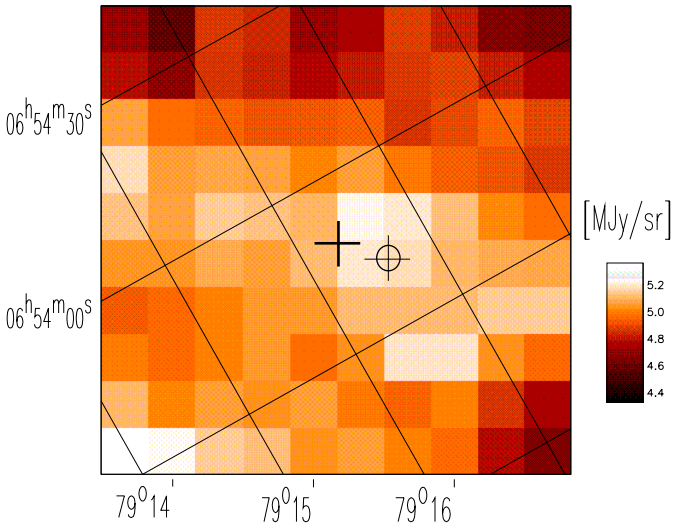

Fig. 3. Merged 60 μm and 90 μm map from November 11, 1997. The OT position is marked with a cross. The local maximum near the position of the OT is marked with a circle. There are other sources near the edge of the map which are brighter but have lower signal to noise due to the lower coverage in those areas.

where λ is the wavelength, I_ν is the background surface brightness level and a telescope of diameter 60 cm is assumed (Helou & Beichman, 1990). The validity of the formula is discussed in Herbstmeier et al. (1998) , and is probably better than an order of magnitude. The detection limit also depends on the absolute calibration of the background surface brightness. The maps indicate background surface brightness levels in the range 3-6 MJy/sr which correspond to cirrus confusion noise fluxes of N(60 μm) $\sim$ 1.5–4.4 mJy and N(90 μm) $\sim$ 5.6–15.8 mJy. These numbers indicate that most of the noise measured at 90 μm (7 mJy according to Table 1) is probably due to cirrus structures. However, this is not the case at 60 μm. Therefore the noise in the merged 60+90 μm map is higher than the noise in the 90 μm map, contrary to the predicted weighted uncertainty if the noise is purely statistical. The presence of cirrus structures at 90 μm therefore imposes a limit on the signal to noise which can be achieved.

6. Discussion

6.1. Origin of the 60 μm emission

Blink comparison of the November 60 μm and 90 μm maps (Fig. 2) indicate a striking similarity in background structure between them. A correlation analysis confirms that there is a structure in the maps (correlation coefficient 0.62) but that the random noise dominates over the intrinsic variations in the background. The surface brightness ratio (in MJy/sr) determined from the maps is consistent with that expected from cirrus in the Galaxy (I90/I60 = 2.03 ± 0.9). It is therefore plausible that the background structures in the maps are due to cirrus. If the 90 μm emission at the position of the GRB is entirely attributed to cirrus, then the maximum cirrus contribution to the flux at 60 μm is $\sim$10 mJy. Subtracting this component from the observed fluxes in May and November, an averaged source flux of 45 ± 18 mJy is obtained. On the other hand, if the 60 μm flux is attributed to cirrus then the flux at 90 μm should be ~ 100 mJy which is clearly not the case. We can thus rule out a Galactic cirrus origin for the source at 60 μm.

A stellar origin for the 60 μm source can also be excluded on the basis that the ISO colours are incompatible with stellar spectra over the full range of spectral types (Smith et al., 1987; Henden & Stone, 1998).

We can also exclude with reasonable confidence the possibility that the 60 μm source is entirely due to transient fireball emission from the GRB on the basis that (a) the flux at 60 μm on May 24 is about two orders of magnitude greater than the extrapolated radio-optical afterglow spectrum on the same date and (b) the source is detected again in November at a consistent flux level (to within 2σ). If the 60 μm emission followed the $t^{-1.1}$ decay of the afterglow, its flux should have decayed by a factor of roughly 15 by November. The relativistic shock scenario accounts quite well for the features of the broadband spectral energy distributions of GRB afterglows and a new physical mechanism, beyond the scope of this paper, would have to be developed if the extraordinary excess at 60 μm was to be connected to the fireball. We now argue instead that the infrared colours we observe in the source are physically reasonable if attributed to conventional dust emission from a single blackbody source.

Modified blackbody spectra of the form $\nu^n \times \mathrm{B}_\nu(\mathrm{T})$, were fit to the range of 60 μm/12 μm colour ratios (R) obtained from observations in May 1997 (Hanlon et al., 1999):

F60 μm=66 mJy/F12 μm=0.065 mJy $\Rightarrow R \sim 1000$
F60 μm=76 mJy/F12 μm=0.035 mJy $\Rightarrow R \sim 2200$
F60 μm=56 mJy/F12 μm=0.095 mJy $\Rightarrow R \sim 600$.

No colour corrections were incorporated in view of the errors on the flux determinations. Estimated temperatures for modified blackbody spectra with $0 < n < 2$ were then obtained for these R values and predicted F90 μm/F60 μm ratios were calculated for each derived dust temperature and assumed emissivity (Table 2). The temperatures for each dust model are well constrained. Moreover, the predicted 90 μm fluxes do not vary significantly for a given n even when R changes by almost a factor of 4. These results also show that subtracting a 10 mJy cirrus component from the 60 μm flux does not significantly affect the conclusion. Since no observations were made at 90 μm in

Table 2. Modified blackbody spectral fits for different values of R, yielding a range of estimated dust temperatures and predicted F90 μm/F60 μm colours. The R values were derived from the May 1997 CAM and PHT data.

R	T_{dust} (K)			Predicted F90 μm/F60 μm		
	$n=0$	$n=1$	$n=2$	$n=0$	$n=1$	$n=2$
600	91	81	70	0.79	0.58	0.44
1000	87	76	68	0.83	0.61	0.45
2200	82	72	65	0.86	0.64	0.47

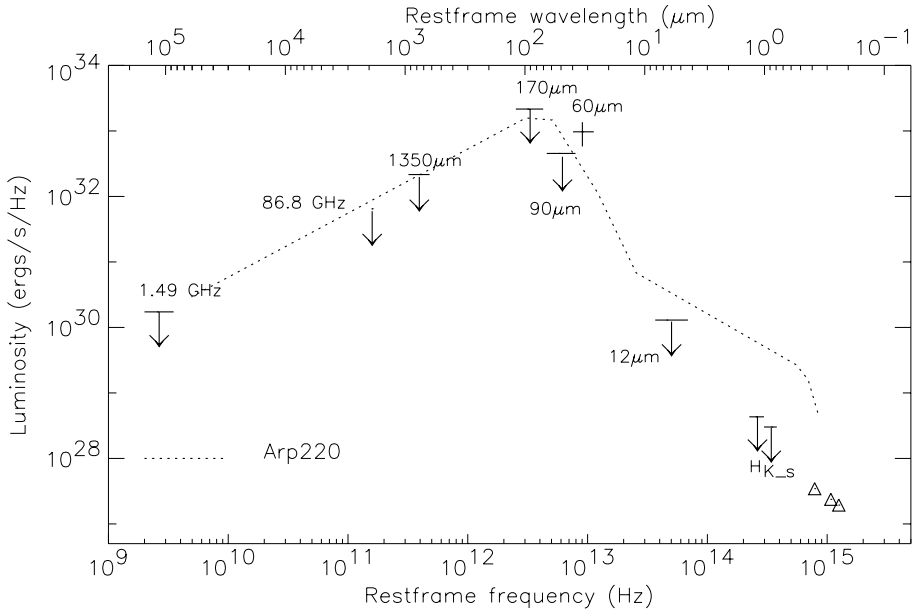

Fig. 4. Spectral energy distribution of the 60μm source, assuming it is the host galaxy of GRB 970508. Data and upper limits are from Bloom et al. 1998; Pian et al. 1998; Smith et al. 1999; Galama et al. 1998; Shepherd et al. 1998 and the present work. The 12 μm upper limit was obtained by co-addition of the 2 CAM LW10 May observations. The C_60 data point represents the averaged flux from May and November. The SED of the ULIG Arp 220 is shown for comparison purposes only.

May 1997, due to orbital constraints, we cannot compare these predicted ratios with observations at the same epoch. However, the fit results can be used to predict the 90 μm flux in November 1997 by appropriate scaling of the 60 μm flux ratios from May (66$\pm$10 mJy) and November (43$\pm$13 mJy). Taking into account the photometric errors, the ratio of the May to November 60 μm flux is in the range 76/30 (2.5) to 56/56 (1). Multiplying the predicted F90 μm/F60 μm ratios in Table 2 by these scaling factors we see that the predicted 90 μm flux for November 1997 is consistent with the observed 90 μm value for all dust models when the scaling factor is 2.5 and for the $n = 2$ case when the scaling factor is 1. Therefore it is not necessary to speculate that the infrared source has varied between the two epochs because the ISO observations are consistent with dust emission from a single blackbody with a temperature of $\sim$ 70 K and $n = 2$. The predicted 170 μm fluxes are always within the upper limits obtained (Table 1), being a factor of two lower than the 90 μm values.

If the 60 μm source is associated with the GRB host galaxy, at a redshift of 0.835, limits can be placed on its bolometric luminosity. A broadband spectral energy distribution (SED) for the 60 μm source, assuming it is the host galaxy of the GRB, is shown in Fig. 4. The assumed cosmological parameters are H_0=50 km s^{-1} Mpc^{-1} and q_0=0.5. If the upper limits across the spectral range are included and the area under the SED is integrated using a power law interpolation between spectral points, an upper limit on the bolometric luminosity (0.4–1000 μm) of $2.9 \times 10^{12} L_\odot$ is obtained. A value of $2.0 \times 10^{12} L_\odot$ is obtained if we consider only the ISO data points and upper limits as contributing towards the luminosity and clearly the emission is dominated by the infrared component. Alternatively, the 60 μm source may be associated with the foreground absorbing system at z=0.767 in which case the infrared luminosity is $\sim 1.7 \times 10^{12} L_\odot$. In either case the source is an ultraluminous infrared galaxy (ULIG, $L_{ir} > 10^{12} L_\odot$) (Sanders & Mirabel, 1996). Although ULIGs were discovered by the IRAS satellite in our local universe (z < 0.2) (Soifer et al., 1986) a recent re-analysis of the IRAS data has shown the existence of ULIGs out to z=0.529 (van der Werf et al., 1999). The extremely rare hyperluminous infrared galaxies (HyLIG, $L_{ir} > 10^{13} L_\odot$) have been detected to z=2.2 (Rowan-Robinson et al., 1991; Cutri et al., 1994).

There are two galaxies within 5″ of GRB 970508, either of which may be responsible for the absorption system seen at z=0.767 (Pian et al., 1998). Due to the large PHT pixel size, it is possible that one of these galaxies, rather than the GRB host, is the counterpart of the 60 μm source. The galaxy to the north-west of the GRB, 'G2' (Pian et al., 1998) has the colours of a late-type spiral at a redshift of 0.7, making it unlikely to be the counterpart, since IRAS detected no late-type spirals with $L_{ir} > 10^{11} L_\odot$ (Sanders & Mirabel, 1996). Galaxy 'G1' to the north-east, has extremely blue colours indicative of a rapidly star-forming system (Pian et al., 1998) and we cannot rule out that it is the counterpart of the 60 μm source.

The prototypical ULIG is Arp 220 with a far-infrared luminosity $> 10^{12} L_\odot$. The SED of Arp 220 (Fig. 4) consists of a cold component, corresponding to a modified blackbody temperature of $\sim$ 50 K and a warm component with a temperature of 120 K peaking shortward of 60 μm (Klaas et al., 1997). It has been suggested that the warm component ($L_{warm} = 10^{11} L_\odot$) is heated by an active nucleus, while the cold component ($L_{cold} = 10^{12} L_\odot$) is starburst powered (Rowan-Robinson & Efstathiou, 1993).

6.2. Probability of a chance superposition

The *a posteriori* probability of finding a 60 μm source within a PHT 41″ diameter beam can be estimated by extrapolating recently determined ISO survey source counts at 15 μm, 90 μm and 170 μm. At 15 μm the integral source counts at 50 mJy from the ELAIS survey are $\sim 10^4$ per steradian while

at 90 μm there are 10^5 to 10^6 sources per steradian to the same flux limit (Rowan-Robinson et al., 1999). In a deep survey of the Lockman Hole, source counts at 95 μm and 170 μm at 150 mJy extrapolate into the same range as ELAIS at 50 mJy (Kawara et al., 1999). The consistency of the source counts from 90 to 175 μm and the increasing source counts from 15 μm to 175 μm indicate that an estimate of $\sim 10^5$ sources per steradian at 60 μm is reasonable. This implies a probability of $\sim 5 \times 10^{-3}$ of finding a 60 μm source down to a detection limit of 50 mJy by chance in a PHT beam of 41″ diameter.

Alternatively, modelled source counts at 60 μm can be used to derive the probability that the 60 μm source is a chance superposition with the GRB host (Pearson & Rowan-Robinson, 1996). Taking into account source counts due to normal, starburst, Seyfert and HyLIGs, the probability of finding a 60 μm source with the observed flux within a PHT beam is also $\sim 5 \times 10^{-3}$. These estimates are sufficiently small to hypothesise a physical connection between the 60 μm source and the host galaxy of the GRB.

6.3. The star formation rate of the 60 μm source

It has long been recognised that some starbursts are obscured by dust (Kennicutt, 1998) and recent results from ISO have shown that such obscuration is widespread and important for the history of star formation in the universe (Elbaz et al., 1999). Hence far-infrared luminosities provide a more reliable estimate of star formation rates in galaxies. If the source is a ULIG, then most of its massive star formation occurs in dense molecular clouds and what is observed at visible frequencies represents emission from stars forming near the edges of clouds which can escape directly without being reprocessed by the dust (Rowan-Robinson et al., 1997). The SFR can be deduced from the far-infrared luminosity using the following expressions for M_*, the rate of star formation per year in units of $M_\odot$: $M_* = 2.6\phi/\epsilon \times \frac{L_{60}}{L_\odot} \times 10^{-10}$ and $M_* = 9.3\phi/\epsilon \times \frac{L_{15}}{L_\odot} \times 10^{-10}$ where ϕ incorporates a correction factor from a Salpeter initial mass function (IMF) to the true IMF and a correction if the starburst is only forming massive stars (Rowan-Robinson et al., 1997). ϵ is the fraction (~ 1) of optical and ultraviolet energy emitted in a starburst (lasting 1 Gyr) which is absorbed by dust and re-emitted in the far infrared. L_{60} and L_{15} are the rest-frame 60 μm and 15 μm luminosities (νL_ν expressed in units of $L_\odot$). These two measures yield values for M_* of between 190ϕ and $220\phi\, M_\odot$/year. An alternative estimate which uses the infrared (8–1000 μm) luminosity and which assumes starbursts lasting $< 10^8$ years, yields a SFR of $\sim 500\, M_\odot$/year (Kennicutt, 1998).

The identification of a ULIG as the possible parent of the GRB host galaxy therefore favours models of GRB formation involving compact stellar remnant progenitors, such as supernovae (Berezinsky et al., 1996; Woosley, 1993) or hypernovae (Paczynski, 1998), which place GRBs in or near star-forming regions. The possible detection of an iron line in the X-ray spectrum of GRB 970508 provides independent support for this scenario (Piro et al., 1999). However, the HST data show that the optical transient is well-centred on the host galaxy, which is quite blue (Fruchter et al., 1999). Since ULIGs tend to be disturbed, dusty systems, with a significant fraction undergoing mergers, the host galaxy would be expected to be redder in colour and its morphology more disturbed than is observed (Clements et al., 1996). Another possibility is that the GRB host has been formed by the ULIG, as the product of a merger. Small galaxies formed along the tidal tails in mergers are likely to detach to become dwarf systems with characteristics (e.g. colour, absolute magnitude) similar to the GRB host (Sanders & Mirabel, 1996; Hunsberger et al., 1996). We can speculate in that case that the offset observed in the May and November 60 μm maps between the 60 μm peak and the OT is genuine, arising from the observation that the most luminous tidal dwarfs are those at the largest projected distances from the parent nucleus (Hunsberger et al., 1996). The galaxy G1 may also have been formed in the merger but a direct redshift determination would be required to support this hypothesis.

7. Conclusions

The ISO observations of GRB 970508 place unique limits on the level of far-infrared emission in the weeks and months following the burst event. Non-transient emission observed at 60 μm indicates the presence of a ULIG which may be the parent of the host galaxy of the GRB. This result may have important implications for GRB progenitor models, favouring those which place GRBs in or near star-forming regions.

Acknowledgements. The ISOPHOT data presented in this paper was reduced using PIA, which is a joint development by the ESA Astrophysics Division and the ISOPHOT consortium. The ISOCAM data presented in this paper was analysed using CIA, a joint development by the ESA Astrophysics Division and the ISOCAM Consortium. The ISOCAM Consortium is led by the ISOCAM PI, C. Cesarsky, Direction des Sciences de la Matiere, C.E.A., France.

References

Berezinsky V., Blasi P., Hnatyk B., 1996, ApJ 469, 311
Bloom J., Djorgovski S., Kulkarni S., Frail D., 1998, ApJ 507, L25
Boella G., Butler R., Perola G., et al., 1997, A&AS 122, 299
Bond H., 1997, IAU Circular, 6654
Bremer M., Krichbaum T., Galama T., et al., 1998, A&A 332, L13
Castro-Tirado A., Metcalfe L., Laureijs R., et al., 1998a, A&A 330, 14
Castro-Tirado A., Gorosabel J., Benítez N., et al., 1998b, Sci 279, 1011
Cesarsky C., Abergel A., Agnèse P., et al., 1996, A&A 315, L32
Chary R., Neugebauer G., Morris M., et al., 1998, ApJ 498, L9
Clements D., Sutherland W., McMahon R., Saunders W., 1996, MNRAS 279, 477
Costa E., Feroci M., Piro L., et al., 1997, IAU Circular, 6649
Cutri R., Huchra J., Low F., et al., 1994, ApJ 424, L65
Delaney M., Hanlon L., Metcalfe L., et al., 1999, in: Cox P., Kessler M. (eds.), The Universe as seen by ISO, p. 1027
Djorgovski S., Metzger M., Kulkarni S., et al., 1997, Nat 387, 876
Elbaz D., Aussel H., Césarsky C., et al., 1999, in: Cox P., Kessler M. (eds.), The Universe as seen by ISO, p. 1031
Frail D., Kulkarni S., Nicastro L., et al., 1997, Nat 389, 261

Frontera F., Costa E., dal Fiume D., et al., 1997, A&AS 122, 357
Fruchter A., Pian E., Gibbons R., et al., 1999, astro-ph/9903236
Gabriel C., Pulido J.A., Heinrichsen I., Morris H., Tai W.M., 1997, in: Hunt G., Payne H. (eds.), ASP Conference Series 125
Galama T., Wijers R., Bremer M., et al., 1998, ApJ 500, L101
Hanlon L., Metcalfe L., Delaney M., et al., 1999, A&AS 138, 459
Heise J., in 't Zand J., Costa E., et al., 1997, IAU Circular 6654
Helou G., Beichman C., 1990, in: Proc. of the 29th Liege International Astrophysics Colloquium
Henden A., Stone R., 1998, AJ 115, 296
Herbstmeier U., Abraham P., Lemke D., et al., 1998, A&A 332, 739
Hunsberger S., Charlton J., Zaritsky D., 1996, ApJ 462, 50
Kawara K., Sato Y., Matsuhara H., et al., 1999, in: Cox P., Kessler M. (eds.), The Universe as seen by ISO, p. 1017
Kennicutt R., 1998, ARA&A 36, 189
Kessler M., Steinz J., Anderegg M., et al., 1996, A&A 315, L27
Klaas U., Haas M., Heinrichsen I., Schulz B., 1997, A&A 325, L21
Klaas U., Kruger H., Heinrichsen I., Heske A., Laureijs R., 1994, ISOPHOT Observer's Manual 3rd ed.
Laureijs R., Klaas U., Richards P., Schulz B., 1998, ISOPHOT Data User's Manual Version 4.0
Lemke D., Klaas U., Abolins J., et al., 1996, A&A 315, L64
Metzger M., Cohen J., Chaffee F., et al., 1997a, IAU Circular, 6676
Metzger M., Djorgovski S., Kulkarni S., et al., 1997b, Nat 387, 878
Paczynski B., 1998, ApJ 494, 45
Pearson C., Rowan-Robinson M., 1996, MNRAS 283, 174
Pian E., Fruchter A., Bergeron L., et al., 1998, ApJ 492, L103
Piro L., Heise J., Jager R., et al., 1998a, A&A 329, 906
Piro L., Costa E., Feroci M., et al., 1998b, A&A 331, L41
Piro L., Costa E., Feroci M., et al., 1999, ApJ 514, 73
Rowan-Robinson M., Broadhurst T., Lawrence A., et al., 1991, Nat 351, 719
Rowan-Robinson M., Efstathiou A., 1993, MNRAS 263, 675
Rowan-Robinson M., Mann R., Oliver S., et al., 1997, MNRAS 289, 490
Rowan-Robinson M., Oliver S., Efstathiou A., et al., 1999, in: Cox P., Kessler M. (eds.), The Universe as seen by ISO, p. 1011
Sanders D., Mirabel I., 1996, ARA&A 34, 749
Shepherd D., Frail D., Kulkarni S., Metzger M., 1998, ApJ 497, 859
Smith B., Kleinman S., Huchra J., Low F., 1987, ApJ 318, 161
Smith I., Tilanus R., van Paradijs J., et al., 1999, A&A 347, 92
Soifer B., Sanders D., Neugebauer G., et al., 1986, ApJ 303, L41
Sokolov V., Zharikov S., Baryshev Y.V., et al., 1999, A&A 344, 43
van der Werf P., Clements D., Shaver P., Hawkins M., 1999, A&A 342, 665
Woosley S., 1993, ApJ 405, 273